Journal of Applied Polymer Science

Drug-Loaded Polyurethane/Clay Nanocomposite Nanofibers for Topical Drug-Delivery Application

Kasturi Saha, Bhupendra Singh Butola, Mangala Joshi
Department of Textile Technology, Indian Institute of Technology Delhi, New Delhi 110016, India
Correspondence to: M. Joshi (E-mail: mangala@textile.iitd.ac.in)

ABSTRACT: In this study, polyurethane/nanoclay nanocomposite nanofibrous webs were prepared by electrospinning. An antiseptic drug, chlorhexidine acetate (CA), was loaded onto montmorillonite clay and was then incorporated into polyurethane nanofibers. For comparison, the CA drug was loaded directly into the polyurethane solution dope used to electrospin the nanofibers. The emphasis was on investigating the effect of the drug loading into the nanoclay vis-à-vis direct drug loading on the drug-release behavior of nanofibrous webs. The nanofibrous webs were also evaluated for other properties, such as moisture vapor transmission, porosity determination, contact angle measurement, and antibacterial activity, which are important for topical drug-delivery application.
 J. Appl. Polym. Sci. **2014**, *131*, 40230.

KEYWORDS: biomedical applications; clay; drug-delivery systems; electrospinning; polyurethanes

Received 30 August 2013; accepted 30 November 2013
DOI: 10.1002/app.40230

INTRODUCTION

Recently, electrospinning has generated a lot of interest in producing nanofibers with a diameter of less than 1 μm.[1] Because of the large surface-area-to-volume ratio and the high porosity of the electrospun webs, they have been targeted for applications in the area of filtration,[2] biosensors,[3] nanocomposites,[4] electrical (electrostatic dissipation, corrosion protection, electromagnetic interference shielding, photovoltaic device, fabrication of tiny electronic devices, e.g., Schottky junctions and actuators),[5] protective clothing for defense and security,[6] cosmetics,[7] enzyme immobilization,[8] and various biomedical applications.[9,10] The biomedical applications of nanofibers mainly focus on the areas of tissue engineering, wound healing, drug delivery, small-diameter vascular graft implants, healthcare, and the biotechnology sector. A review of recent patents related to electrospun nanofibers revealed that around two-thirds[11] of all such applications are in the biomedical field.

Drug delivery via electrospun nanofibers has gained much attention because of the possibility of delivering uniform, large, and controlled doses of pharmaceutical agents at the action site via a high surface-area-to-volume ratio, high porosity, and high flexibility of the lightweight nanofibrous system as compared to conventional drug-delivery systems, such as films and gels. Nanofibrous drug-delivery systems also have many advantages, including a high therapeutic efficiency at a lower dose, reduced toxicity due to the delivery of the drug to the specific action site, availability of a large application area, and minimal adverse effects. Although many studies on the use of nanofibrous systems for the delivery of various antibiotics[12–14] and anticancer drugs[15,16] are available in the literature, no specific work has reported the use of electrospun polymeric nanocomposite fibrous webs where nanoclay has been used as a drug carrier for antibacterial application or an *in vitro* drug-release study.

Medical-grade thermoplastic polyurethane (TPU) has been selected as the polymer of choice for the preparation of nanofibers because of its various advantages, such as its biocompatibility, sterilizability, chemical resistance, excellent strength, tear and wear resistance, and high elastic memory for maintaining tension, and it also provides patient comfort because of its high moisture vapor transmission rate (MVTR), which is essential for breathability and softening at body temperature, which is necessary to maintain its properties. Because of the aforementioned properties, TPU also finds applications[17] in the area of medical devices, including feeding tubes, catheters, vascular grafts, various connector designs, and long-term implants such as pacemakers. In the literature, polyurethane nanofibrous webs find application in drug delivery with various drugs in pure form, such as ketoprofen[18] (a nonsteroidal anti-inflammatory drug), itraconazole (an antifungal drug), and ketanserin (an acute renal failure drug),[19] and tetracycline hydrochloride (an antibiotic).[20] In all these studies, the drug was directly incorporated into the polyurethane nanofiber during the electrospinning stage.

The drug used for this study was chlorhexidine acetate (CA), a cationic antiseptic that acts as both a bacteriostatic and a

bactericidal agent.[21] This biguanide antibiotic has been established in the treatment of the nosocomial transmission of infections, skin and mucosal infection caused by the bacteria. It also acts as an antiseptic, pharmaceutical and cosmetic preservative, and antiplaque agent. Chlorhexidine-containing formulations are used[22] for urinary or central venous catheter impregnation as well. There was a recent report[22] on polyurethane in film form containing chlorhexidine diacetate drug for dental application.

Montmorillonite (Mt) nanoclay is an important member of the smectite family and has been used as a carrier for the cationic CA drug in TPU nanofibers. The interlayer spacings of Mt are generally occupied by various exchangeable cations, such as Na^+, K^+, Ca^{2+}, Mg^{2+}, and water moieties; this explains the high cation exchange (70–120 mequiv./100 g) capacity of this type of clay mineral. Mt clay has large specific surface area, colloidal properties, good absorbability, adhesive ability, and drug carrying capability. The unique crystalline structure of Mt clay allows the expansion and contraction of the interlayer spacing by substitution with various organic and inorganic cationic species to form intercalation composites.[23] Thus, Mt is one of the most extensively used minerals,[24] both as an excipient and active substance, in the pharmaceutical industry.

In this study, modified montmorillonite nanoclay loaded with chlorhexidine acetate drug (CAMt) was created with an ion-exchange reaction as per details given in our previous publication.[25] The nanofibrous nonwoven webs containing the pure drug (CA) and CAMt were electrospun separately under optimized process conditions. The morphology of the electrospun nanofibers was studied by scanning electron microscopy (SEM). The electrospun nanofibers containing the drug and drug-loaded clay were further characterized by X-ray diffraction (XRD), contact angle measurement, porosity determination, and MVTR analysis. The antimicrobial activity of the drug-loaded fiber and nanocomposite fiber was determined against both Gram-positive and Gram-negative bacteria. The *in vitro* release of the drug from the electrospun nanofiber in phosphate-buffered saline (PBS; pH 7.4) media at 37°C was investigated to study the effect of the nanoclay on the drug-release kinetics. These bioactive nanofibers have the potential for application in the area of controlled topical drug delivery and will be particularly useful in applications such as wound dressing.

EXPERIMENTAL

Materials

Aromatic polyether-based TPU (TEXIN RxT85A, weight-average molecular weight = 540,615 Da, as measured by gel permeation chromatography with a polystyrene standard) was procured from Bayer Material Science LLC (Pittsburgh, PA). Sodium Mt clay with a cation-exchange capacity of 1.20 mequiv/g was procured from Southern Clay Products, Inc. (Japan) and was used without further treatment.

CA (white powder, molecular weight = 625.55, mp = 156°C, solubility = 1.49 mg/mL in water at 25°C) was obtained from Sigma-Aldrich Co., Ltd. (Dorset, United Kingdom) and was used as received. The chemical structure ($C_{22}H_{30}Cl_2N_{10}{\cdot}2C_2H_4O_2$) of the model drug is shown in Figure 1.

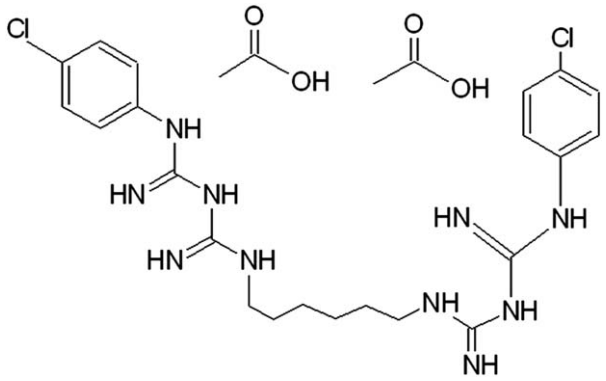

Figure 1. Chemical structure of the CA drug.

Sodium chloride (NaCl), potassium chloride (KCl), disodium hydrogen phosphate (Na_2HPO_4), potassium dihydrogen phosphate (KH_2PO_4), and dimethylformamide (DMF) were purchased from Merck, India.

Preparation of the Polymer Dope

TPU solution was prepared by the dissolution of TPU chips in DMF with a magnetic hot plate with a stirrer (Schott Instruments, Germany) at 70°C and 250 rpm for 4 h to obtain a clear solution of 10% w/w TPU.

In the first case, CA with concentrations of 1 and 5% w/w of the 10% dry weight of TPU was added to a small amount of DMF individually, and these samples were subjected to ultrasonic treatment (37 KHz) for 30 min at room temperature. The drug solution was then added to the TPU solution and stirred at 250 rpm for two h at a temperature of 70°C before electrospinning.

In the second case, the drug-loaded clay, that is, CAMt, at concentrations of 1 and 5% w/w of the 10% dry weight of TPU was added to a small amount of DMF individually, and these samples were also subjected to ultrasonic treatment (37 KHz) for 120 min at room temperature (25°C). In the 1 and 5% CAMt, the amount of CAMt was such that the drug concentration (i.e., that of CA) was kept 1 and 5% w/w, respectively, with respect to the 10% dry weight of the TPU dope. This CAMt solution was then added to the TPU solution separately and stirred at 250 rpm for two h at 70°C before electrospinning. The compositions of the various prepared TPU–drug solutions are listed in Table I.

Preparation of the Electrospun Nonwoven Nanofibrous Mat

An electrospinning machine (Nanomate IP 607,TSPL Hyderabad, India) consisting of a syringe with a blunt-end metal needle, an infusion syringe pump for controlling the feed rate, a grounded stainless steel plate collector, and a high-voltage power supply unit was used. The neat polymer solution and the polymer solutions containing the drug and drug-loaded clay were transferred to a 5-mL syringe having a 0.26-mm inner diameter needle (Gauge-25). Various parameters were standardized to prepare monolithic nanofibers from the polymeric solutions. The electric field strength was maintained in the range

Table I. Composition of the Various TPU–Drug Solutions as Prepared

Abbreviation	Composition
TPU-1% CA	1% w/w CA dissolved in 10% TPU solution
TPU-5% CA	5% w/w CA dissolved in 10% TPU solution
TPU-1% CAMt	1% w/w CA-Mt dissolved in 10% TPU solution
TPU-5% CAMt	5% w/w CA-Mt dissolved in 10% TPU solution

10–25 kV. A uniform pressure was applied to the syringe solution to maintain a steady feed rate in the range 5–30 μL/min. The tip-to-collector distance was adjusted between 5 and 10 cm. During the electrospinning process, the temperature and relative humidity were maintained in the range 22–25°C and 46–50%, respectively.

After a series of standardizations, the optimized process parameters were obtained, as summarized in Table II. The electrospun fiber mats were dried overnight in a vacuum chamber at room temperature to evaporate the residual solvent from the nanofibers and were stored at 4°C.

Nanofiber Characterization

Morphological Analysis. The surface morphologies of the nanofibrous webs were investigated with a scanning electron microscope (model Zeiss EVO 50) at an accelerating voltage of 20 kV. The SEM samples were coated with gold before the analysis. The SEM photographs were analyzed by ImageJ Software to determine the average diameter of the nanofibers produced. Ten different fibers and 50 different segments were randomly selected from each image to determine the average fiber diameter with this software.

XRD Analysis. XRD studies of all of the nanofibrous webs and Mt nanoclay were carried out on a PaNalytical X-ray powder diffractometer with Ni-filtered Cu Kα radiation with a wavelength of 1.5418 Å, a working voltage of about 40 kV, and a working current of about 30 mA. Scanning was carried out in the 2θ range 2–15° at a scanning rate of 2°/min.

Contact Angle Measurement

Contact angle measurements were done to study the influence of the pure drug and drug-loaded clay on the surface properties of the TPU nanofibrous webs. The water contact angle was measured at room temperature with a DSA 100 contact angle instrument from Krüss (Germany). The sessile drop method was used to determine the contact angle every 5 and 10 s after the water droplet contacted the surface of each nanofibrous sample. For each sample, five droplets of water on the surface were used to obtain the average of 10 readings for each sample, and the average value was recorded for further analysis.

Table II. Optimized Process Parameters for Electrospinning

Composition	Applied voltage (kV)	Feed rate (μL/min)	Tip-to-collector distance (cm)
Neat TPU	15	5	10
TPU-1% CA	15	5	10
TPU-5% CA	15	5	10
TPU-1% CAMt	20	5	10
TPU-5% CAMt	20	5	10

MVTR and Porosity Determination. The MVTR of the electrospun web sample was measured with a PERMATRAN-W (model 101K, Mocon). The MVTR measurement gave us an idea about the transmission rate of water vapor through the porous nanofibrous samples. Test cells containing nanofibrous sample with a thickness of 0.33 mm were used. The sample specimens were conditioned, and the measurements were made in a standard laboratory atmosphere (37 ± 1°C and 65% relative humidity) conditions. The water vapor transmission rate is expressed in units of grams per square meter per day.

The porosity of the electrospun web samples was determined with a capillary flow porometer (model CFP-1100 AEX). A low-surface-tension fluid, Galwik (surface tension = 16 dyne/cm), was used as a wetting medium in the measurement of the pore size of the nanofibrous webs.

Disc Diffusion Test. The antibacterial activities of the nanofibrous samples were tested against both Gram-positive (*Staphylococcus aureus*) and Gram-negative bacteria (*Escherichia coli*) by the disc diffusion test (AATCC 90). Twenty milligrams of electrospun web was placed in a UV chamber for 30 min to sterilize it. Nutrient agar solution was made by the suspension of 20 g of Luria broth in 1000 mL of deionized water, and 15 g of agar–agar was added in the solution as a solidifying agent. After sterilization, about 25–30 mL of nutrient agar solution was uniformly spread on Petri dishes. Ten microliters of bacterial solution was evenly spread over the nutrient agar solution. *S. aureus* and *E. coli* concentrations of approximately 1.2×10^6 and 1.5×10^6 CFU/mL, respectively, were used for these experiments. The sterilized samples were then placed on the nutrient agar plate. The agar plates were kept for incubation at 37°C for 24 h. The zone of inhibition was measured after a 24-h incubation period.

Drug-Release Study. ***Preparation of the PBS solution.*** PBS solution was chosen to simulate the pH of chronic wound exudate at pH 7.4. The ionic concentration and osmolarity of the PBS solution also matched that of the human body. To prepare 1000 mL of the saline solution, 8 g of sodium chloride, 0.20 g of potassium chloride, 1.44 g of disodium hydrogen phosphate, and 0.24 g of potassium dihydrogen phosphate were dissolved in about 800 mL of distilled water. The pH value of the saline solution was verified with a pH meter (model PHAN, Labindia Analytical) and was adjusted to 7.4 by the addition of sodium hydroxide. Finally, 200 mL of distilled water was added to the solution to increase the volume to 1000 mL.

In vitro *release study.* The drug-release behavior of TPU–CA and TPU–CAMt (1 and 5%) nanocomposite fibers was studied in PBS solution at pH 7.4 by the total immersion method. About 10 mg of nanofiber was taken and put in different conical flasks, with each containing 10 mL of buffer solution; these were then tightly capped and placed in an incubation chamber

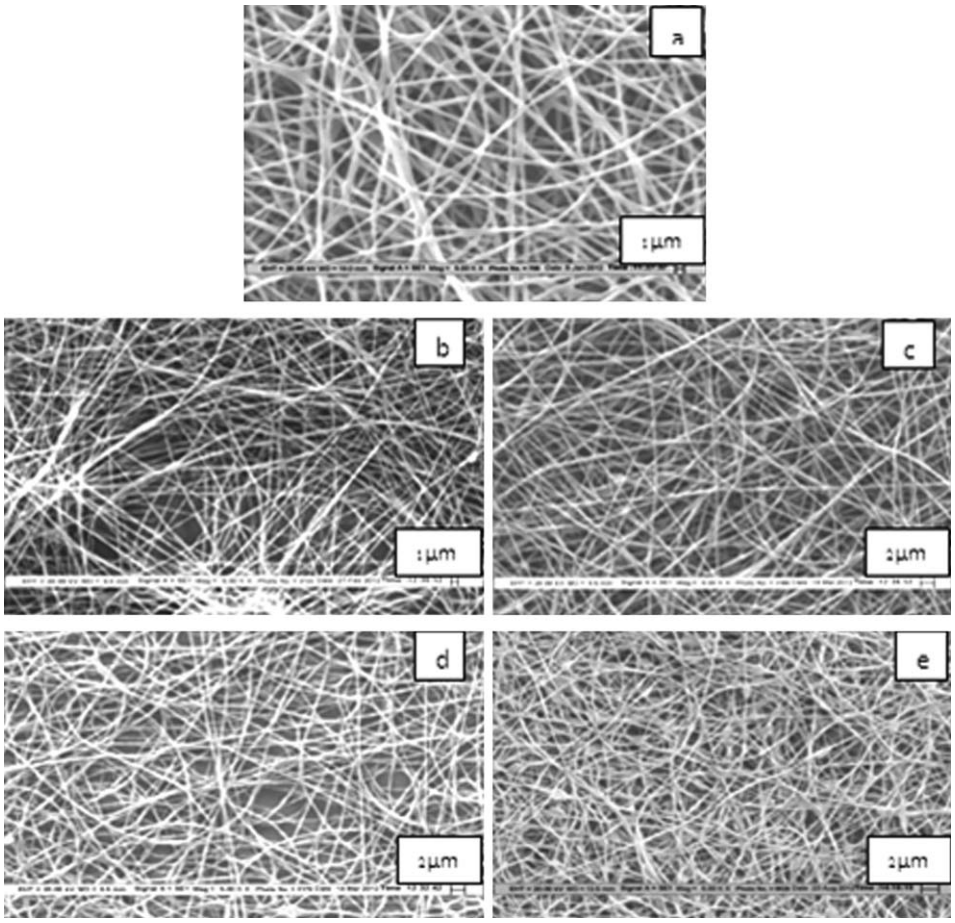

Figure 2. SEM images of the (a) neat TPU and TPU containing (b) 1% CA, (c) 5% CA, (d) 1% CAMt, and (e) 5% CAMt.

at 37 ± 0.1°C with stirring at 200 rpm to study the release profile of the CA drug. About 2 mL of the solution was taken out at specific time intervals, and the corresponding absorbance value was determined in a UV spectrophotometer (PerkinElmer Lambda 25) at Lambda max (λ_{max}) = 254 nm, which was the characteristic peak of CA drug. The cumulative drug concentration was calculated from the calibration curve of the model drug prepared with a CA solution of known concentrations in PBS solution (pH 7.4). The tests were performed in triplicate, and the results were recorded as an average of three readings.

RESULTS AND DISCUSSION

Morphological Analysis

Figure 2 shows selected SEM images of the as-spun TPU nanofibers. Clearly, round cross-section fibers with smooth surfaces were obtained, and no drug crystals were detected on the surface of the nanofibers. These SEM images indicate that the drug was finely incorporated into the electrospun fibers.

Figure 2(a) corresponds to the SEM images of the neat TPU nanofiber. The standardized process parameters are described in another section. The nanofibers were collected onto a flat-plate collector with aluminum foil. The average diameter of these fibers was about 410 ± 30 nm.

Figure 2(b,c) shows to the SEM images of the drug-loaded TPU (1 and 5%) nanofibers, respectively. We obtained a homogeneous distribution of the nanofibers with optimum diameter by maintaining the same process conditions as were used for the neat TPU. The average diameter of these fibers ranged between 350 and 370 nm.

The SEM images of the TPU nanofibers containing drug-loaded clay (1 and 5%) are shown in Figure 2(d,e). During the fabrication of this kind of nanofiber, a higher voltage was applied to obtain a homogeneous distribution of diameter ranging between 325 and 375 nm.

XRD Analysis

The XRD patterns of the Mt nanoclay, neat TPU, and TPU containing the drug and drug-loaded clay in the form of nanofibrous webs are shown in Figure 3.

The XRD pattern of the neat TPU and CA drug-loaded TPU web did not exhibit any characteristic peaks. However, the 1 and 5% CAMt loaded TPU webs exhibited two distinct peaks at positions of 3.82 and 7.43° with interlayer spacings of 23.05 and 11.92 Å, respectively. The first peak corresponded to the successful drug intercalation into the clay intergallery with the increase in interlayer spacing. On the other hand, the second

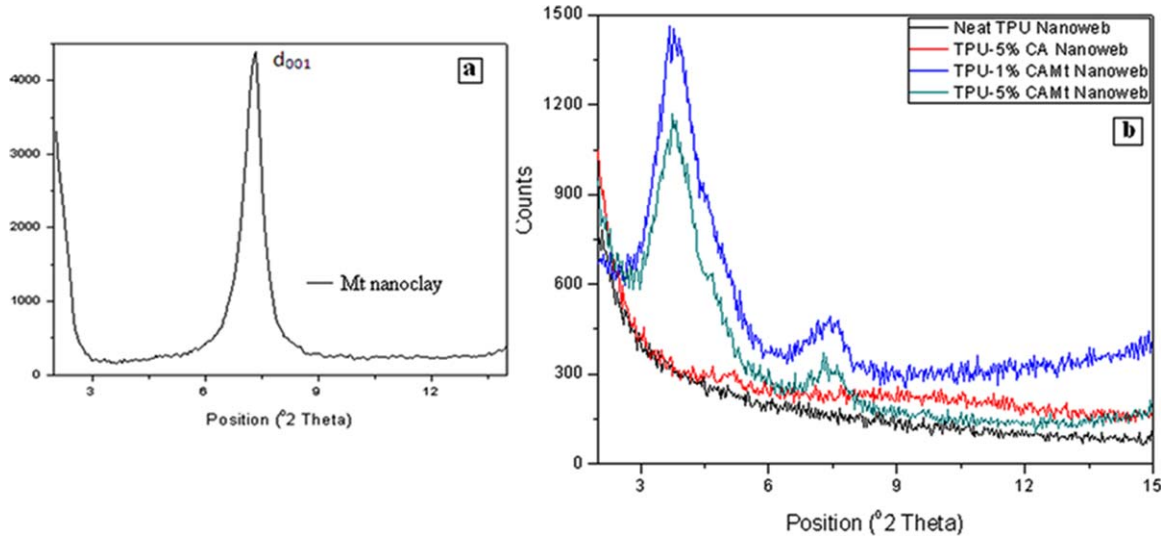

Figure 3. XRD pattern of the (a) Mt nanoclay and (b) neat TPU, TPU–CA, and TPU–CAMt nanofibrous web. [Color figure can be viewed in the online issue, which is available at wileyonlinelibrary.com.]

one represents a characteristic measure of the distance between planes of atoms in a crystalline lattice obtained through XRD technique (d_{001}) peak for the crystalline sodium Mt clay mineral.[25] Therefore, we concluded that the drug-loaded clay was successfully incorporated into the electrospun nanofibrous web. Although the CA drug was crystalline in nature, it remained homogeneously distributed into the nanofibrous web and, therefore, did not exhibit any characteristic peaks in the X-ray diffractogram.

Contact Angle Measurement

The water contact angle values after the droplet contacted the electrospun nanofibrous samples are shown in Figure 4.

In the literature,[26] it was mentioned that TPU films exhibit a contact angle of 76°; this indicates that TPU itself is somewhat hydrophilic in nature. Figure 4(a) shows a water droplet on the surface of the TPU nanofibrous web for the measurement of the water contact angle. However, interestingly, the measured water contact angle for the neat TPU mat reached 101.1 ± 1.7° after electrospinning; this indicated a hydrophobic nature. This was due to the higher surface roughness and lower contact point available for the electrospun nanofibrous sample as compared to a TPU film.

On the other hand, the contact angle value for the drug-loaded electrospun fibrous mat [Figure 4(b)] was larger (116.3 ± 1.3°) than that of the corresponding neat TPU mats. This was because of the hydrophobic character of the CA drug. Again, the contact angle value slightly decreased (111.5 ± 1.6°) for the CAMt–TPU [Figure 4(c)] electrospun mat, perhaps because of the hydrophilic nature of the clay.

MVTR and Porosity Determination

The MVTRs for the neat TPU web and nanofibrous web containing the drug and drug-loaded clay (5%) is shown in Figure 5.

Figure 5 shows that a higher MVTR was obtained in case of the TPU nanofibers in comparison with the nanofibrous webs containing the drug and drug-loaded clay. A higher MVTR value indicated that there was a greater passage of moisture vapor through the material. We expected that this decreased the moisture vapor transmission in the CA and CAMt-incorporated nanofibrous web would be helpful in maintaining wound moisture and preventing dehydration; this is necessary for successful wound healing, and it can also control the water loss from a wound at an optimal rate. The results of MVTR were in agreement with the mean pore diameters of the neat TPU, TPU–CA, and TPU–CAMt nanofibrous webs, which are presented in Table III. The neat TPU nanofibers exhibited a higher MVTR value compared to the others, as its mean pore size was higher compared to the TPU–CA and TPU–CAMt nanofibrous webs.

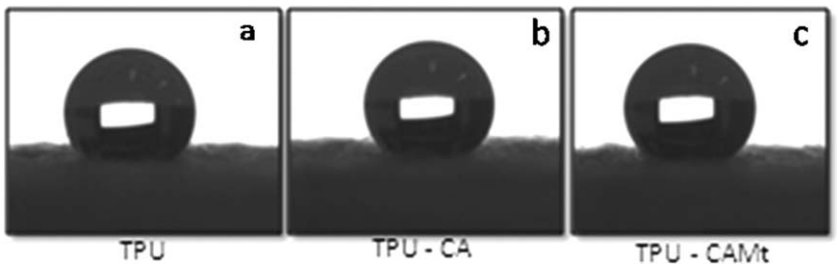

Figure 4. Contact angle images of the (a) neat TPU, (b) TPU–CA, and (c) TPU–CAMt nanofibrous web.

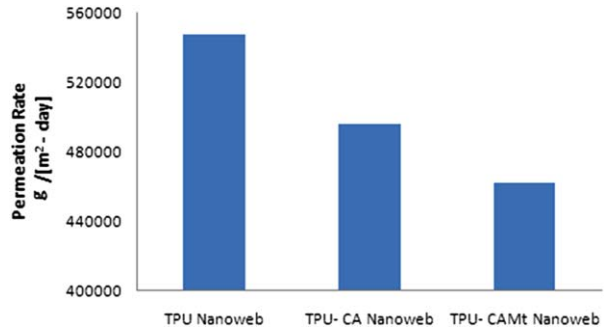

Figure 5. Bar diagram for the MVTR measurements of the neat TPU, TPU–CA, and TPU–CAMt nanofibrous web. [Color figure can be viewed in the online issue, which is available at wileyonlinelibrary.com.]

Disc Diffusion Test

The disc diffusion test results of the various nanofibrous web samples are shown in Figure 6 and 7. Neat TPU showed no inhibitory zone for *S. aureus* and *E. coli*; this reflected no antibacterial activity [Figure 6(a) and 7(a)]. However, the electrospun nanofibrous samples loaded with pure CA drug and CAMt (1 and 5%) showed a very clear zone of inhibition around the specimen, as shown in Table IV.

Table III. Pore Size of the Neat TPU, TPU–CA, and TPU–CAMt Nanofibrous Webs

Sample	Mean pore diameter (μm)
TPU nanoweb	0.722
TPU-CA nanoweb	0.581
TPU-CAMt nanoweb	0.357

These results indicate that both the CA- and CAMt-loaded electrospun samples had strong activity against both the Gram-positive and Gram-negative bacteria. The presence of a

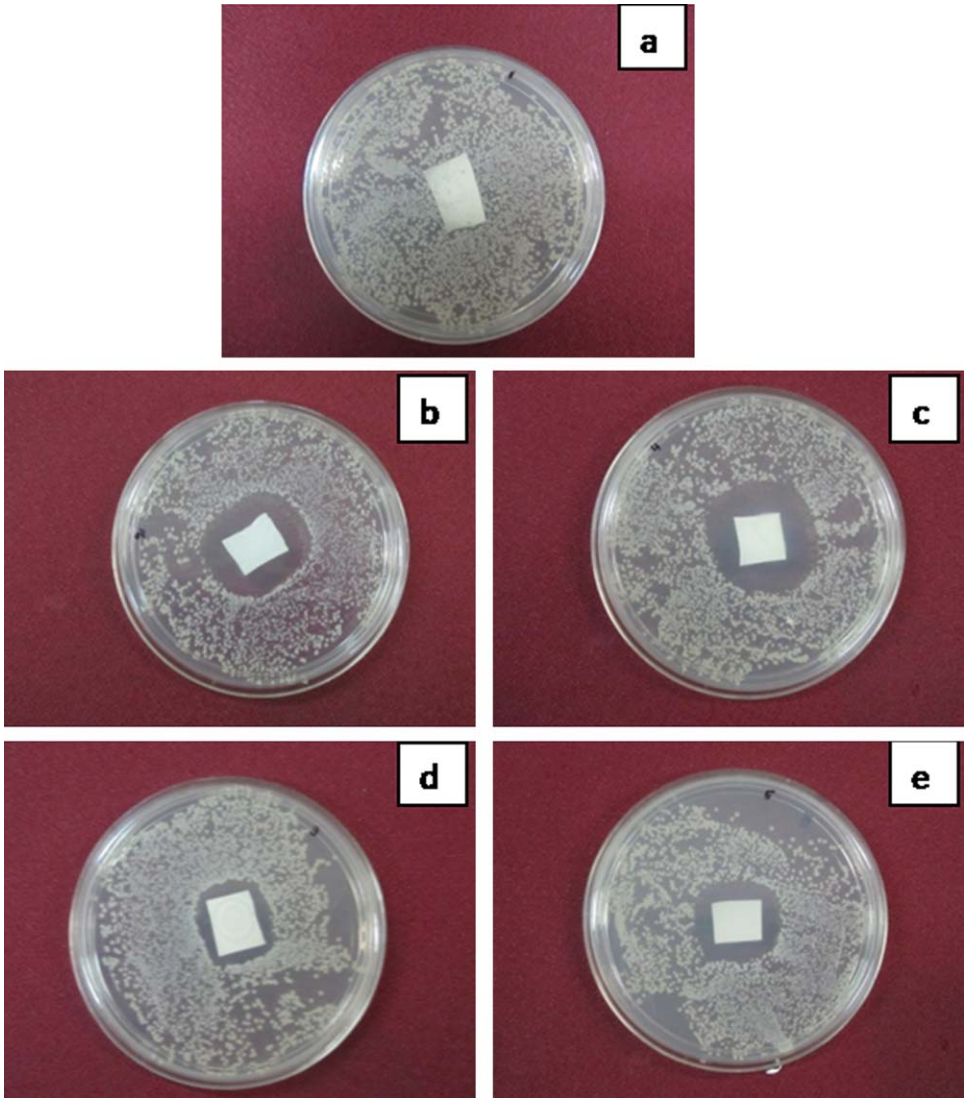

Figure 6. Photograph showing the zone of inhibition of the (a) neat TPU and TPU nanofibrous web containing (b) 1% CA, (c) 5% CA, (d) 1% CAMt, and (e) 5% CAMt against *S. aureus*. [Color figure can be viewed in the online issue, which is available at wileyonlinelibrary.com.]

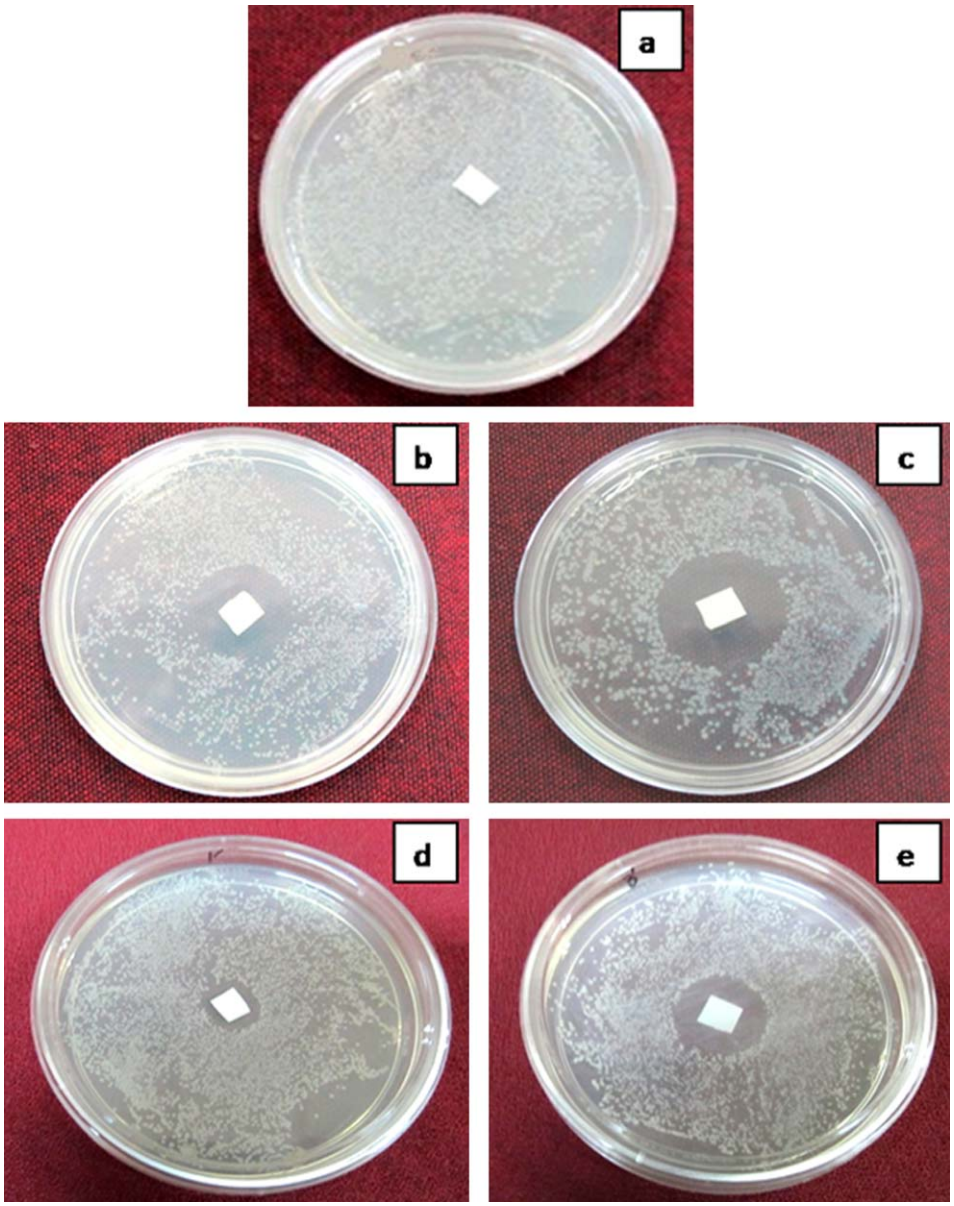

Figure 7. Photograph showing a zone of inhibition of the (a) neat TPU and TPU nanofibrous web containing (b) 1% CA, (c) 5% CA, (d) 1% CAMt, and (e) 5% CAMt against *E. coli*. [Color figure can be viewed in the online issue, which is available at wileyonlinelibrary.com.]

zone of inhibition was an indication of the diffusion of an antibacterial agent from modified Mt into the agar. It was clear that with increasing concentrations of CA and CAMt in the nanofibrous webs, the zone of inhibition increased. However, the pure-drug (CA)-loaded nanofibrous web samples showed a larger zone of inhibition compared to the CAMt-loaded nanofibrous samples. This was due to the higher diffusion rate of the pure drug into the agar as compared to the drug that was intercalated into the clay intergalleries in the case of CAMt.

Table IV. Inhibition Zone of the Neat TPU and TPU Web Containing CA and CAMt against *S. aureus* and *E. coli* Bacteria

	Zone of inhibition (in mm)	
	S. aureus	*E. coli*
Neat TPU	Absent	Absent
TPU-1% CA	33	32
TPU-5% CA	37	35
TPU-1% CAMt	25	23
TPU-5% CAMt	28	28

The mechanism responsible for the antibacterial activity of the CA[27] drug is the electrostatic attraction forces between the cationic CA drug and the negatively charged bacterial cell wall. The drug molecule disrupted the integrity of the cell membrane after absorption onto the microorganism's cell wall and caused the outflow of intracellular components of the microorganisms. As a result of this, the microorganisms gradually died, and this resulted in a clear zone of inhibition.

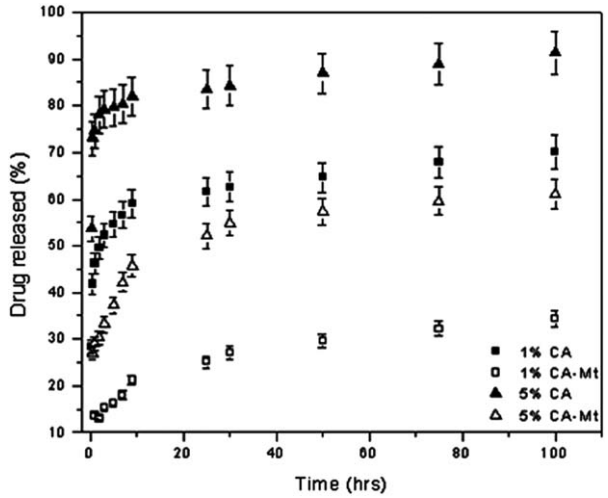

Figure 8. Release profile of the pure drug CA and CAMt nanofibrous webs in PBS media at pH 7.4 and 37°C.

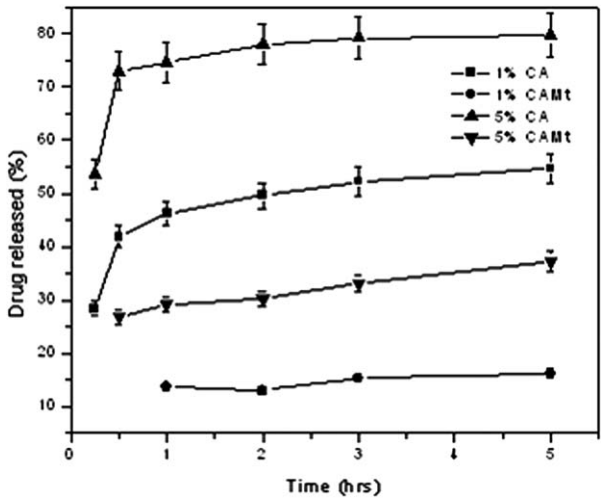

Figure 9. Release profile of the CA and CAMt nanofibrous webs for an initial 5 h.

In Vitro Release Study

The cumulative amounts of drug released (reported as the percentage of the actual amount of drug present in the drug-loaded samples) from the pure-drug- and CAMt-nanocomposite-loaded nonwoven webs in a PBS media at pH 7.4 and 37°C are shown in Figure 8 and 9.

From the figure, it was obvious that the drug from nanofibrous web was continuously released for over 100 h. A large amount of pure CA drug release corresponded to the well-known burst effect, which was observed in the first 5 h and was followed by a slower release thereafter from the nanofibrous webs. The amount of drug released increased monotonically with increasing initial drug loading from 1 to 5% in the TPU nanofiber. On the basis of the release profile at pH 7.4, the maximum release of 91% of the pure drug was observed in case of the 5% drug-loaded nanofiber, whereas for the 1% drug-loaded nanofibers, a maximum of only 70% release was obtained. However, 100% drug release was never attained because of the equilibrium characteristics of the ion-exchange reaction responsible for drug release.

In the case of the CAMt-loaded TPU nanofiber, the initial burst release effect was diminished (Figure 9). Here, the drug started to release after a time lag; that is, in the case of the 1% CAMt-loaded nanofiber, it took 60 min, whereas in the case of the 1% CA nanoweb, it only took 30 min. This kind of sustained release occurred because of the presence of bulky and hydrophobic drug cations being immobilized into the interlayer spacing, which could not be deintercalated easily[28] by the ion-exchange reaction with the small Na^+, K^+ cations present in the intergallery. Only 16 and 37% of the drug were released during the initial 5 h from the 1 and 5% CAMt-loaded nanofiber samples, respectively. After that, the drug-release rate remained almost constant for about 100 h in a sustained manner compared to the pure drug. The maximum release of the drug from the 1 and 5% CAMt was observed in the range of 35 and 65%, respectively; as compared to the respective 70 and 91% in case of the 1 and 5% CA incorporated nanofibrous webs.

Therefore, we concluded that the nanofibrous web containing drug loaded via intercalation into the clay interlayer spacing had a positive effect in terms of the release behavior. The pure-drug-loaded nanofiber exhibited burst release followed by first-order release kinetics, where the drug-release rate was proportional to the drug concentration. This kind of burst release is advantageous for the treatment of bacterial colonization and infection-related diseases where immediate action is necessary. However, for long-term activity, this burst release characteristic is not beneficial. On the other hand, the TPU nanofibrous web containing drug loaded onto the clay interlayer spacing exhibited sustained release characteristics with zero-order kinetics. For a drug-delivery carrier, this kind of release kinetics is beneficial where long-term activity is desirable.

CONCLUSIONS

TPU containing the drug (CA) and drug-loaded clay (CAMt) in the form of nanofibrous webs were successfully prepared by the electrospinning technique. The morphology of the electrospun fiber, as studied by SEM, showed a smooth surface and uniform beadless nanofibers under the optimized process conditions. The contact angle value showed an increase, whereas the MVTR diminished in the case of the nanofibrous web containing the drug and drug-loaded clay as compared to the neat nanofiber. This would be useful for maintaining wound moisture and preventing dehydration during wound healing.

The antibacterial assay showed that both the CA and CAMt loaded nanofibrous webs had broad-spectrum antibacterial activity against both the Gram-positive and Gram-negative bacteria. The drug-release profile of the nanofibrous web containing pure drug into PBS media indicated burst release, whereas the intercalated species exhibited sustained release activity. The drug-release kinetics depended on both the initial drug concentration and also on the immobilization of the drug onto the clay mineral vis-à-vis pure drug incorporation in the nanofibrous webs. Moreover, both types of drug release obeyed the Fickian diffusion mechanism, but they transformed from burst

to sustained nature after drug intercalation into the clay interlayer spacing. Such sustained release is useful in topical drug delivery and in wound healing with long-term activity, and these are a potential applications for these TPU–CA and TPU–CAMt nanofibrous webs.

ACKNOWLEDGMENTS

The authors thank Lockheed Martin Corp. and Advanced Technology Laboratories (NJ) for sponsoring this project under the Nano Biological Research Program.

REFERENCES

1. Zhou, F.; Gong, R. *Polym. Int.* **2008**, *57*, 837.
2. Tsaia, P. P.; Schreuder, G. H.; Gibson, P. *J. Electrostat.* **2002**, *54*, 333.
3. Li, D.; Frey, M. W.; Baeumner, A. J. *J. Membr. Sci.* **2006**, *279*, 354.
4. Maruyama, B.; Alam, K. *SAMPE J.* **2002**, *38*, 59.
5. Norris, I. D.; Shaker, M. M.; Ko, F. K.; Macdiarmid, A. G. *Synth. Met.* **2000**, *114*, 109.
6. Schreuder, G. H.; Gibson, P.; Senecal, K.; Sennett, M.; Walker, J.; Yeomans, W. *J. Adv. Mater.* **2002**, *34*, 44.
7. Smith, D.; Reneker, D. H.; Schreuder, G. H.; Mello, C.; Sennett, M.; Gibson, P. PCT US00/27776 (**2001**).
8. Jia, H.; Zhu, G.; Vugrinovich, B.; Kataphinan, W.; Reneker, D. H.; Wang, P. *Biotechnol. Prog.* **2002**, *18*, 1027.
9. Dersch, R.; Steinhart, M.; Boudriot, U.; Greiner, A.; Wendorff, H. *J. Polym. Adv. Technol.* **2005**, *16*, 276.
10. Agarwal, S.; Wendorff, J. H.; Greiner, A. *Polymer* **2008**, *49*, 5603.
11. Burger, C.; Hsiao, B. S.; Chu, B. *Annu. Rev. Mater. Res.* **2006**, *36*, 333.
12. Bolgen, N.; Vargel, I.; Korkusuz, P.; Menceloglu, Y. Z.; Piskin, E. *J. Biomed. Mater. Res. B Appl. Biomater.* **2007**, *81*, 530.
13. Huang, Z. M.; He, C. L.; Yang, A.; Zhang, Y.; Han, X. J.; Yin, J. *J. Biomed. Mater. Res. A* **2006**, *77*, 169.
14. Kim, K.; Luu, Y. K.; Chang, C.; Fang, D.; Hsiao, B. S.; Chu, B. *J. Controlled Release* **2004**, *98*, 47.
15. Xu, X.; Chen, X.; Xu, X.; Lu, T.; Wang, X.; Yang, L. *J. Controlled Release* **2006**, *114*, 307.
16. Xie, J.; Wang, C. H. *Pharm. Res.* **2006**, *23*, 1817.
17. Kutay, S.; Tincer, T.; Hasirci, N. *Brit. Polym. J.* **1990**, *23*, 267.
18. Kenawy, E. R.; Abdel-Hay, F. I.; El-Newehy, M. H.; Wnek, G. E. *Mater. Chem. Phys.* **2009**, *113*, 296.
19. Geert, V.; Iksoo, C.; Joel, R.; Jef, P.; Alex, V. D.; Jurgen, M.; Marc, N.; Marcus, E. B. *J. Controlled Release* **2003**, *92*, 349.
20. Hong, Y.; Fujimoto, K.; Hashizume, R.; Guan, J.; Stankus, J. J.; Tobita, K.; Wagner, W. R. *Biomacromolecules* **2008**, *9*, 1200.
21. Russell, A. D. *Infection* **1986**, *14*, 212.
22. Huynh, T. T. N.; Padois, K.; Sonvico, F.; Rossi, A.; Zani, F.; Pirot, F.; Doury, J.; Falson, F. *Eur. J. Pharm. Biopharm.* **2010**, *74*, 255.
23. Lin, F. H.; Lee, Y. H.; Jian, C. H. *Biomaterials* **2002**, *23*, 1981.
24. Wang, X.; Du, Y.; Luo, J. *Nanotechnology* **2008**, *19*, 1.
25. Saha, K.; Butola, B. S.; Joshi, M. *Appl. Clay Sci.*, submitted.
26. Ochoa-Putnam, C.; Vaidya, U. K. *Compos. A* **2011**, *42*, 906.
27. McDonnell, G.; Russell, A. D. *Clin. Microbiol. Rev.* **1999**, *12*, 147.
28. Jung, H.; Kim, H. M.; Choy, Y. B.; Hwang, S. J.; Choy, J. H. *Int. J. Pharm.* **2008**, *349*, 283.